*Manuscript
Click here to view linked References

*J. Eur. Ceram. Soc.*
2017.5.7
Major revision

# Spherical porous granules in $MgO–Fe_2O_3–Nb_2O_5$ system: *In situ* observation of formation behavior using high-temperature confocal laser-scanning microscopy

Yoshikazu Suzuki,[a*] Hiroya Abe[b], Hajime Yamamoto[b], Kazuhiro Ito[b], Hiroshige Inoue[b], Mayumi Nakamura[c]
[a] Faculty of Pure and Applied Sciences, University of Tsukuba, 1-1-1 Tennodai, Tsukuba, Ibaraki, 305-8573, Japan
[b] Joining and Welding Research Institute, Osaka University, 11-1 Mihogaoka, Ibaragi, Osaka 567-0047, Japan
[c] Yonekura MFG Co., 2-11-5, Shin-Yokohama, Kohoku, Yokohama, Kanagawa, 222-0033, Japan

## Abstract

The pyrolytic reactive granulation process, yielding ceramic spherical porous granules, is simple, consisting of typical ceramic processing methods, *viz.*, wet-ball milling of powders, vacuum drying, granulation via sieving through a screen mesh, and one-step heat treatment for local reactive sintering within each granule. Here, the microstructural development of spherical porous granules was successfully visualized by *in situ* high-temperature confocal laser-scanning microscopy during the heating up to 1400°C in air. Based on the result of the *in situ* observation, a simple but powerful size-controlling process of spherical porous granules, *viz.*, multiscreen sieving after the heating was demonstrated. Nearly monodispersed spherical porous granules composed of pseudobrookite-type $MgFeNbO_5$ were easily obtained.

***Keywords***: spherical porous granule (SPG), *in situ* observation, confocal laser-scanning microscopy (CLSM), pseudobrookite, $MgFeNbO_5$

## 1. Introduction

Spherical porous granules (SPGs) are promising for many applications, *e.g.*, heterogeneous catalysts, catalyst supports, drug delivery carriers, healing of defective bones and so on [1-8]. A variety of processes have been developed to form SPGs; they are mostly liquid-based processes, particularly spray drying [1,2], suspension hardening [3,4], drop-in-oil [5], sol-gel granulation [6] and freeze-granulation [2,7]. Solid-based processes are rarely realized for the SPG production, except the mechanical granulation method with a rotating fluidized bed [8]. Recently, we have reported a new solid-based process to synthesize SPGs by a one-step heat-treatment of the $MgCO_3$(basic)-α-$Fe_2O_3$-$Nb_2O_5$ mixed powder. Pseudobrookite-type $MgFeNbO_5$ SPGs with 3-D

* Corresponding Author
E-mail: suzuki@ims.tsukuba.ac.jp
Tel: +81-29-853-5026 / Fax: +81-29-853-4490

network structure, typically 50-100 μm in diameter, were successfully obtained (Fig. 1) [9].

This pyrolytic reactive granulation (PRG) process is really simple, consisting only of typical ceramic processes, *viz.*, wet-ball milling of starting powders, vacuum drying, granulation via sieving through a screen mesh, and a simple heat treatment (without pressing). Nevertheless, this new mechanical and solid-based process yields porous granules with relatively high sphericity [9]. This PRG process is similar to the pyrolytic reactive sintering process used to obtain bulk porous ceramics [10-12]; emitted $CO_2$ or $H_2O$ gas in starting carbonates, hydroxides etc. formed a uniformly open porous 3-D network structure with pore diameter of ~1 μm. The final diameter (typically 50-100 μm) of SPGs by the pyrolytic reactive granulation is probably governed by the opening size of sieving mesh (< 150 μm) used in the powder process before the heating.

Previously [9], microstructure development during heating was investigated with *ex situ* (i.e., ordinary) SEM observation for the samples after heating at intermediate temperatures. With an *ex situ* SEM observation, dynamic microstructure development cannot be followed. *In situ* high-temperature (HT) microscopy is effective to dynamically pursue the microstructure development during the heating. Depending on the sample size/shape and the required resolution, optical microscopy (OM), scanning electron microscopy (SEM) [13-15], transmission electron microscopy (TEM) [16-18] and scanning probe microscopy (SPM) [19] have been combined with HT observation. Recently, confocal laser-scanning microscopy (CLSM), an advanced type of optical microscopy, can be utilized for the HT observation, where an infrared image furnace enables the HT observation up to as high as 1800°C in air. The HT-CLSM is increasingly being used in metallurgy and ceramic fields [20-23].

Here the primary purpose is to clarify the microstructural development during the heating of SPGs by using the HT-CLSM. The secondary purpose, based on the outcome from the HT-CLSM, is to develop a facile size-control method for SPGs.

## 2. Experimental

### *2.1. Materials*

As before [9], commercially available $MgCO_3$ (basic) (hydromagnesite, $Mg_5(CO_3)_4(OH)_2{\bullet}4H_2O$, 99.9%, Kojundo Chemical Laboratory), α-$Fe_2O_3$ and $Nb_2O_5$ (99.9% each, Wako Pure Chemical Ind.) powders were used as the starting materials. Prior to the weighing, TG-DTA analysis (up to 1000 °C) on the $MgCO_3$ (basic) powder was conducted to determine the weight-loss during the heating. The $MgCO_3$ (basic), α-$Fe_2O_3$ and $Nb_2O_5$ powders (Mg:Fe:Nb = 1:1:1 in mole fraction) were wet-ball milled for 24 h in ethanol with $ZrO_2$ balls, vacuum dried and sieved through 100 mesh screen (<150 μm).

### *2.2. In situ high-temperature observation*

A confocal laser scanning microscope using a 408 nm violet laser (VL2000DX, Lasertec, Japan) equipped with a high-temperature *in-situ* observation system is used with an infrared image furnace (SVF17SP, Yonekura, Japan, as shown in Fig. S1). The $Mg_5(CO_3)_4(OH)_2•4H_2O$ $–Fe_2O_3–Nb_2O_5$ mixed powder in a small alumina crucible (6.5 mmϕ) was observed up to 1400°C under flowing air with a ramp rate of 100°C/min for R.T.-800°C and 20°C/min for 800-1400°C.

*2.3. Synthesis and size control of spherical porous granules*

The $Mg_5(CO_3)_4(OH)_2•4H_2O–Fe_2O_3–Nb_2O_5$ mixed powder in an alumina crucible was heated to 1300°C in a box furnace (ramp rate: 5°C/min) with 30 min holding at the maximum temperature. The temperature of the furnace was verified using TempCHEK pellets (Orton, USA). The constituent phases of SPGs were analyzed by X-ray diffraction (XRD, Cu-Kα, 40 kV and 40 mA, Multiflex, Rigaku, Japan). Quantitative composition analysis of the Pt-coated SPGs was carried out with SEM-EDS (SU-70, Hitachi / INCA System, Oxford) at the acceleration voltage of 15 kV. Based on the preliminary result of HT-CLSM observation, we decided to use multiple screens for the classification of spherical porous granules (Fig. 2); it is an old-fashioned way, but is really cost effective and compatible with industrial powder processes. Using 3 meshes with different openings (150, 100 and 75 μm), SPGs were classified with manual vibration for ~5 min. The classified SPGs were observed by SEM, and their diameter values (500 granules for each sample) were determined by image analysis using Image-J software.

**3. Results**

*3.1. In situ high-temperature observation*

Figure 3 shows the microstructure development of SPGs observed by HT-CLSM. Percentages in photos show the diameter change of a selected granule during the heating. Shrinkage of the granules is clearly observed from 120 to 900°C, which is mainly attributed to the pyrolysis of $Mg_5(CO_3)_4(OH)_2•4H_2O$. At around 1100-1300°C, the sphericity improves caused by the reactions and rearrangements of the constituent grains, in particular for larger granules. The $MgFeNbO_5$ porous granules retained their spherical shape up to ~1350°C (with gradual densification), but began to be consolidated at ~1400°C due to local eutectic liquid phase formation. The *in situ* high-temperature observation clearly demonstrates the size change during the pyrolytic reactive granulation, which suggests that the classification (unification of the size) of rigid $MgFeNbO_5$ SPGs should be much easier after heating than that of soft agglomerates before heating.

*3.2. Synthesis and size control of SPGs*

Figure 4 shows an XRD pattern of SPGs, showing almost single-phase pseudobrookite-type $MgFeNbO_5$ with a trace of spinel phase, as seen in the previous work [9]. Some isolated intermediate,

but rather stable, spinel grains co-existed in the porous structure. Figure 5 shows a result of SEM-EDS wide-area analysis of an $MgFeNbO_5$ SPG. Semi-quantitative analysis using INCA software indicated that the SPG was composed of 11.6 at.% Mg, 11.9 at.% Fe, 12.1 at.% Nb and 64.5 at.% O, which are close to the ideal composition of 12.5 at % of each metal and 62.5 at % of oxygen. Note that the estimated error by Pt coating is less than 1 at.% in this study. The uniformly open-porous structure is composed of somewhat elongated grains with irregular shapes as commonly observed for pseudobrookite-type ceramics.

Figure 6 shows SEM micrographs and particle-size distributions for SPGs after multiscreen classification/sampling: (a) between 100 and 150 μm openings (sample A), and (b) between 75 and 100 μm openings (sample B). Due to the mild manual vibration/sieving, some finer granules still remained for both samples in Fig. 6. However, nearly monodispersed granules can be easily obtained by such an "old-fashioned" but versatile method. Note that some granules with ellipsoid-like or irregular morphologies passed through the mesh possessed somewhat larger sphere-equivalent diameters. It is also noteworthy that, as is seen in HT-CLSM, larger granules tend to have better sphericity, which is confirmed by the aspect ratio analysis.

The BET surface area of samples A and B were 0.52 $m^2/g$ and 0.57 $m^2/g$, respectively. These values are similar to those of bulk UPC-3D (uniformly porous ceramics with 3-D network structure) as before [10,11].

## 4. Discussion

### *4.1. Microstructure development of SPGs*

For the *ex situ* SEM observation [9], sample preparation steps (*e.g.* fixation of granules on carbon tape using a spatula) somewhat affected the macroscopic sample shapes, particularly for the soft granules. After the pyrolysis of $Mg_5(CO_3)_4(OH)_2{\bullet}4H_2O$ phase (*i.e.*, MgO nanoparticle formation) at intermediate temperatures, the mechanical strength of the granules seems be weak, and hence, the macroscopic sample shapes can be easily collapsed. A major advantage of the *in situ* method, as here, is that it avoids a deformation of the shapes of granules during the preparation necessary in the *ex-situ* method [9]. Another advantage is to avoid the secondly atmosphere effect of $H_2O$ and $CO_2$ in air reacting with *e.g.* MgO nanoparticles,

The diameter of a selected granule (Fig. 3) decreased by 50-60% of the initial size. This shrinkage for SPG was more extensive than that for bulk green samples with pre-pressing. Without macroscopic liquid phase formation, each granule can unrestrictedly deform. Based on the *in situ* HT-XRD [9] and the HT-CLSM analyses in this study, the microstructure development of SPGs during the heating is schematically illustrated in Fig. 7. Even before the heating, the mixed powder was composed of "spherical-like" granules with somewhat large size distribution. During the heating, pyrolysis of $Mg_5(CO_3)_4(OH)_2{\bullet}4H_2O$ occurred, and thus, the granules were shrunk. Formation of

intermediate binary oxides ($MgNb_2O_6$ (ss), $MgFe_2O_4$ (ss) and $FeNbO_4$ (ss)) and ternary oxide ($MgFeNbO_5$) helped to rearrange the grain networks, and thereby improved the macroscopic sphericity. Up to 1350°C, without macroscopic liquid phase formation, the porous granules retained their spherical shapes.

*4.2. Size control of SPGs*

As is stated in Section 3.1, the classification (unification of the size) of rigid $MgFeNbO_5$ SPGs with 3-D network structure after the heating should be much easier than that of soft agglomerates of the mixed powder before the heating. It is demonstrated (Fig. 6) that some SPGs by furnace heating (not by the *in situ* observation) had the diameter of ~150 μm, which implies the size shrinkage under the slower heating rate became milder. Formation of the 3-D network structure may result in such mild shrinkage (or even expansion) during the heating [24].

*4.3. Potential applications of SPGs*

Although the base compound, $MgTi_2O_5$, does not show high catalytic activity (except photocatalytic activity), these ternary compounds, $MgFeNbO_5$ and $MgFeTaO_5$ (as originally reported by Bayer [25]) may be useful as redox catalysts. The specific surface area of the SPGs is relatively small, but the spherical granular shape with open pores should be favorable for heterogeneous catalysis. Moreover, $MgFeNbO_5$ SPGs might be applied for biomaterials because $MgFeNbO_5$ is composed only of biocompatible elements.

## 5. Conclusions

We have attempted in this study (1) to clarify the microstructural development during the heating of SPGs by using the HT-CLSM, and (2) to develop a facile size-control method of SPGs. Thus,

(1) The size and morphological change of SPGs during heating was successfully observed by *in situ* HT-CLSM. At around 1100-1300°C, the sphericity seems to be quite improved caused by the reactions and rearrangements of the constituent grains, in particular for larger granules.

(2) The classification via multiscreen sieving for the rigid $MgFeNbO_5$ SPGs after heating was effective for the size-unification. This very simple, old-fashioned technique enabled nearly monodispersed SPGs.

## Acknowledgements

This work was supported by JSPS KAKENHI Grant Number JP16H04212 for Basic Research: Category B, and Joint Research Project of JWRI, Osaka University. We thank to Dr. Peter E. D. Morgan to improve the language.

**References**

[1] H. W. Chang, K. Okuyama, Optical properties of dense and porous spheroids consisting of primary silica nanoparticles, J. Aerosol Sci. 33 (2002) 1701-1720.

[2] E. Garcia, J. Mesquita-Guimarães, P. Miranzo, M.I. Osendi, Porous mullite and mullite-$ZrO_2$ granules for thermal spraying applications, Surf. Coat. Tech. 205 (2011) 4304-4311.

[3] W. Paul, C.P. Sharma, Development of porous spherical hydroxyapatite granules: application towards protein delivery, J. Mater. Sci. Mater. Med. 10 (1999) 383-388.

[4] V.S. Komlev, S.M. Barinov, E.V. Koplik, A method to fabricate porous spherical hydroxyapatite granules intended for time-controlled drug release, Biomaterials 23 (2002) 3449-3454.

[5] S.G. Deng, Y.S. Lin, Granulation of sol-gel-derived nanostructured alumina AIChE J. 43 (1997) 505–514.

[6] Y.K. Nakamura, T.N. Murakami, N.Y. Iwata, Y. Hirano, Y. Tokuoka, N. Kawashima, Preparation of porous diopside microspheres from spherical silica gels impregnated with $Ca(NO_3)_2$ and $MgCl_2$, J. Ceram. Soc. Jpn. 112 (2004)133–137.

[7] F. Paul, J.R. Binder, H. Gesswein, H.J. Ritzhaupt-Kleissl, J.Hausselt, Synthesis of doped $Ba_{0.6}Sr_{0.4}TiO_3$ ceramic powder via a sol–freeze-granulation and freeze-drying process, Ceram. Int. 35 (2008) 479–486.

[8] S. Watano,Y. Imada, K. Hamada,Y. Wakamatsu, Y. Tanabe, R.N. Dave, R. Pfeffer, Microgranulation of fine powders by a novel rotating fluidized bed granulator, Powder Technol. 131 (2003) 250–255.

[9] Y. Suzuki, H. Tokoro, H. Abe, Self-organized formation of spherical porous granules only by one-step heat-treatment in MgO-$Fe_2O_3$-$Nb_2O_5$ system, Mater. Lett. 163 (2016) 43-46.

[10] Y. Suzuki, P. E. D. Morgan, T. Ohji, New uniformly porous $CaZrO_3$/MgO composites with three-dimensional network structure from natural dolomite, J. Am. Ceram. Soc. 83 (2000) 2091-2093.

[11] Y. Suzuki and M. Morimoto, Uniformly porous $MgTi_2O_5$ with narrow pore-size distribution: *in situ* processing, microstructure and thermal expansion behavior, J. Ceram. Soc. Jpn. 118 (2010) 1212-1216.

[12] Y. Suzuki, T. S. Suzuki, Y. Shinoda, and K. Yoshida, Uniformly porous $MgTi_2O_5$ with narrow pore-size distribution: XAFS study, improved in-situ synthesis, and new *in-situ* surface coating, Adv. Eng. Mater. 14 (2012) 1134-1138.

[13] B. Schmid, N. Aas, O. Grong, R. Odegard, High-temperature oxidation of nickel and chromium studied with an in-situ environmental scanning electron microscope, Scanning 23 (2001) 255-266.

[14] G.G.E. Seward, D.J. Prior, J. Wheeler, S. Celotto, D.J.M. Halliday, R.S. Paden, M.R. Tye, High-temperature electron backscatter diffraction and scanning electron microscopy imaging techniques: in-situ investigations of dynamic processes, Scanning 24 (2002) 232-240.

[15] A.J. Smith, H.V. Atkinson, S.V. Hainsworth, A.C.F. Cocks, Use of a micromanipulator at high temperature in an environmental scanning electron microscope to apply force during the sintering of copper particles, Scripta Mater. 55 (2006) 707-710.

[16] M.L. No, A. Ibarra, A. Lopez-Echarri, E.H. Bocanegra, J. San Juan, Diffusion processes in Cu-Al-Ni shape memory alloys studied by mechanical spectroscopy and in situ transmission electron microscopy at high temperatures, Mater. Sci. Eng. A 442 (2006) 418-422.

[17] H. Kruger, V. Kahlenberg, V. Petricek, F. Phillipp, W. Wertl, High-temperature structural phase transition in $Ca_2Fe_2O_5$ studied by in-situ X-ray diffraction and transmission electron microscopy, J. Solid State Chem., 182 (2009) 1515-1523.

[18] J. Bezjak, A. Recnik, B. Jancar, P. Boullay, I.R. Evans, D. Suvorov, High-temperature transmission electron microscopy and X-ray powder diffraction studies of polymorphic phase transitions in $Ba_4Nb_2O_9$, J. Am. Ceram. Soc. 92 (2009) 1806-1812.

[19] D. Varandani, K. Agarwal, J. Brugger, B.R. Mehta, Scanning thermal probe microscope method for the determination of thermal diffusivity of nanocomposite thin films, Rev. Sci. Instrum. 87 (2016) 084903.

[20] M. Reid, D. Phelan, R. Dippenaar, Concentric solidification for high temperature laser scanning confocal microscopy, ISIJ Int. 44 (2004) 565-572.

[21] S.S. Jung, I. Sohn, Effect of FeO Concentration on the crystallization of high-temperature $CaO$-$Al_2O_3$-$MgO$-$FeO$ Melts, J. Am. Ceram. Soc. 96 (2013) 1309-1316.

[22] P. Yan, Y.J. Jeong, M. F. Islam, P. C. Pistorius, Real time and in situ observation of graphene growth on liquid metal surfaces via a carbon segregation method using high-temperature confocal laser scanning microscopy, RSC Adv. 6 (2016) 101235-101241.

[23] I. Sohn, R. Dippenaar, In-situ observation of crystallization and growth in high-temperature melts using the confocal laser microscope, Metal. Mater. Trans. B 47 (2016) 2083-2094.

[24] Y. Nakagoshi and Y. Suzuki, Dimensional change behavior of porous $MgTi_2O_5$ in reactive sintering, Ceram. Int., in press http://dx.doi.org/10.1016/j.ceramint.2017.01.079

[25] G. Bayer, Thermal Expansion Characteristics and stability of pseudobrookite-type compounds, $Me_3O_5$, J. Less Common Met. 24 (1971) 129-138.

**Figure Captions**

**Fig. 1** SEM images of (a) the $Mg_5(CO_3)_4(OH)_2•4H_2O$–α-$Fe_2O_3$–$Nb_2O_5$ mixed powder and (b) its heat-treated-only product (SPGs) at 1350°C; (c) digital optical microscope image of SPGs. Reproduced with permission from [9] with the license No. 4032800187654. Copyright 2016 Elsevier.

**Fig. 2** Multiple screens for the classification of spherical porous granules.

**Fig. 3** Microstructure development of spherical porous granules (SPGs) observed by *in situ* high-temperature confocal laser-scanning microscopy (HT-CLSM). Percentages in photos show the diameter change of a selected granule during the heating.

**Fig. 4** XRD pattern of spherical porous granules, showing almost single-phase $MgFeNbO_5$ with trace spinel phase.

**Fig. 5** SEM-EDS wide-area analysis of a $MgFeNbO_5$ SPG, showing 11.6 at.% Mg, 11.9 at.% Fe, 12.1 at.% Nb and 64.5 at.% O, which are close to the ideal composition of $MgFeNbO_5$: 12.5 at % of each metal and 62.5 at % of oxygen.

**Fig. 6** SEM micrographs, particle-size distributions and aspect ratio for spherical porous granules (SPGs) after multiscreen classification: (a) sampling from the screens between 100 and 150 μm openings, and (b) sampling from the screens between 75 and 100 μm openings.

**Fig. 7** Schematic illustration of the microstructure development during the heating.

# Spherical porous granules in $MgO–Fe_2O_3–Nb_2O_5$ system: *In situ* observation of formation behavior using high-temperature confocal laser-scanning microscopy

Yoshikazu Suzuki,[a*] Hiroya Abe[b], Hajime Yamamoto[b], Kazuhiro Ito[b], Hiroshige Inoue[b], Mayumi Nakamura[c]
[a] Faculty of Pure and Applied Sciences, University of Tsukuba, 1-1-1 Tennodai, Tsukuba, Ibaraki, 305-8573, Japan
[b] Joining and Welding Research Institute, Osaka University, 11-1 Mihogaoka, Ibaragi, Osaka 567-0047, Japan
[c] Yonekura MFG Co., 2-11-5, Shin-Yokohama, Kohoku, Yokohama, Kanagawa, 222-0033, Japan

## Supplement

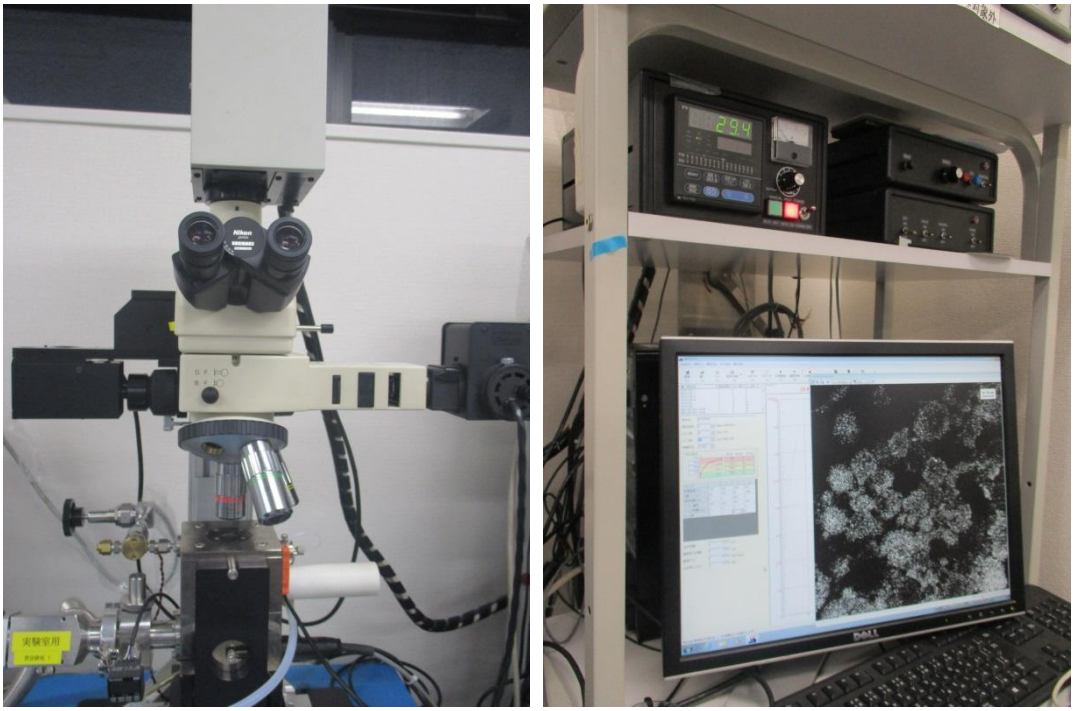

**Fig. S1** Appearance and controller of a high-temperature confocal laser-scanning microscope.

* Corresponding Author
E-mail: suzuki@ims.tsukuba.ac.jp
Tel: +81-29-853-5026 / Fax: +81-29-853-4490

**Figure1**

**Click here to download high resolution image**

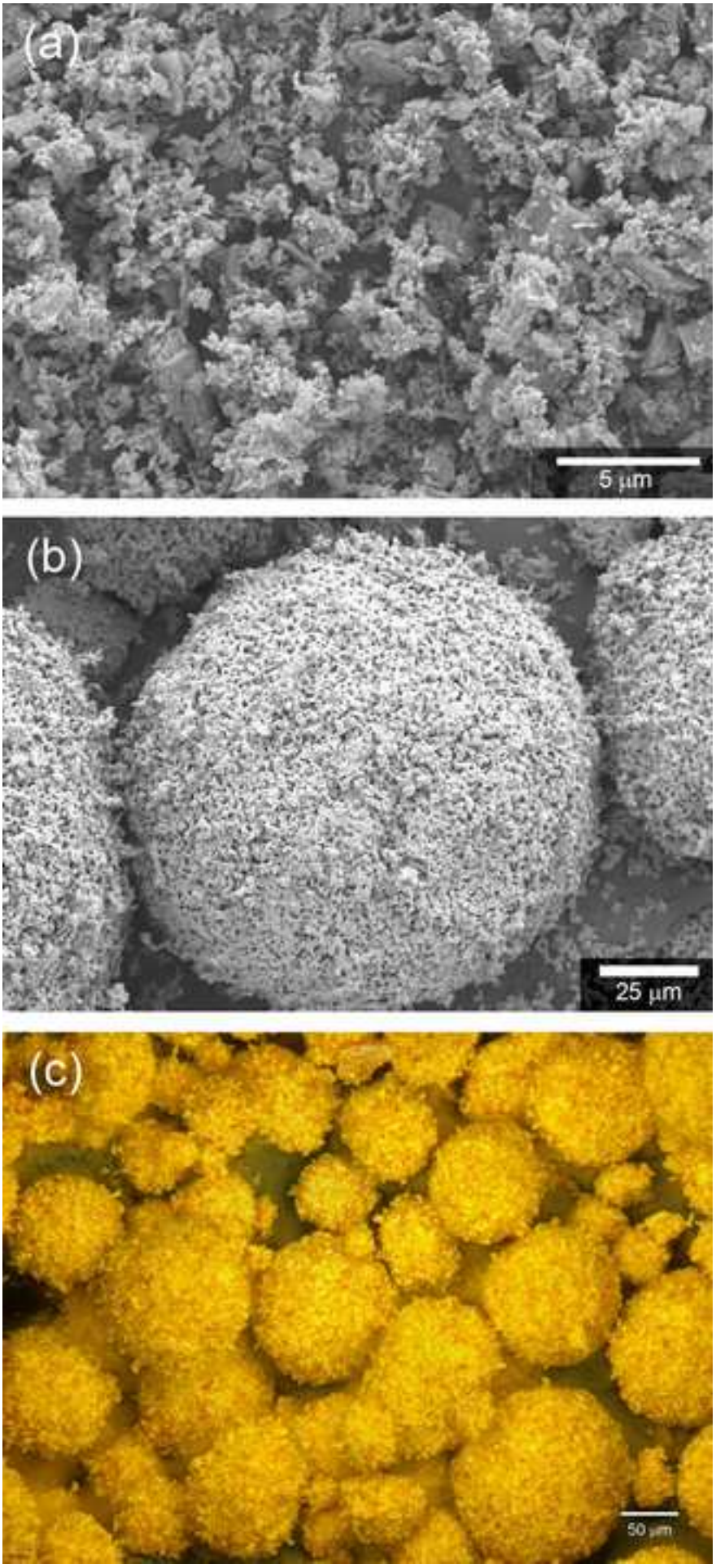

Figure2
Click here to download high resolution image

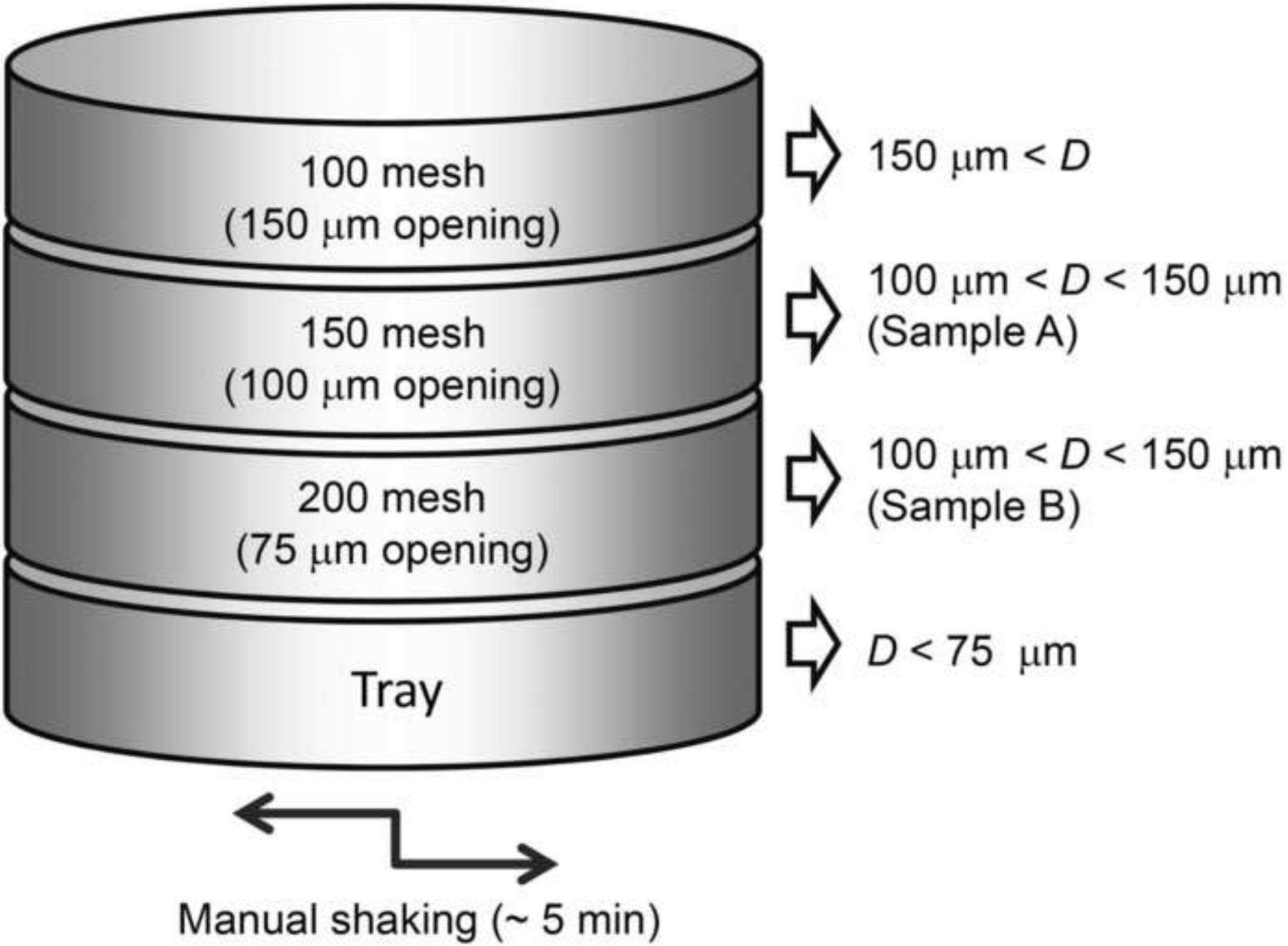

**Figure3**

**Click here to download high resolution image**

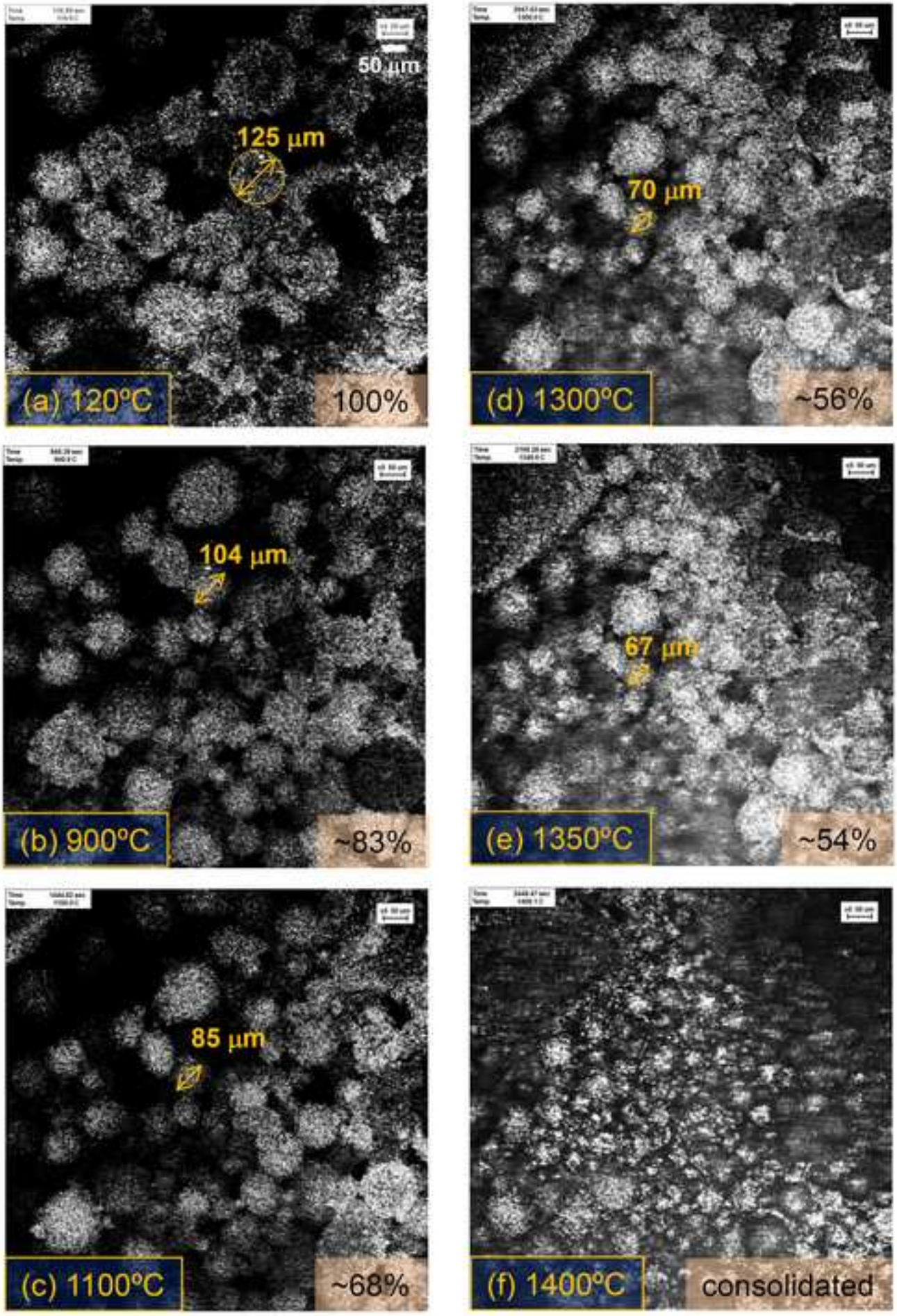

Figure4

Click here to download high resolution image

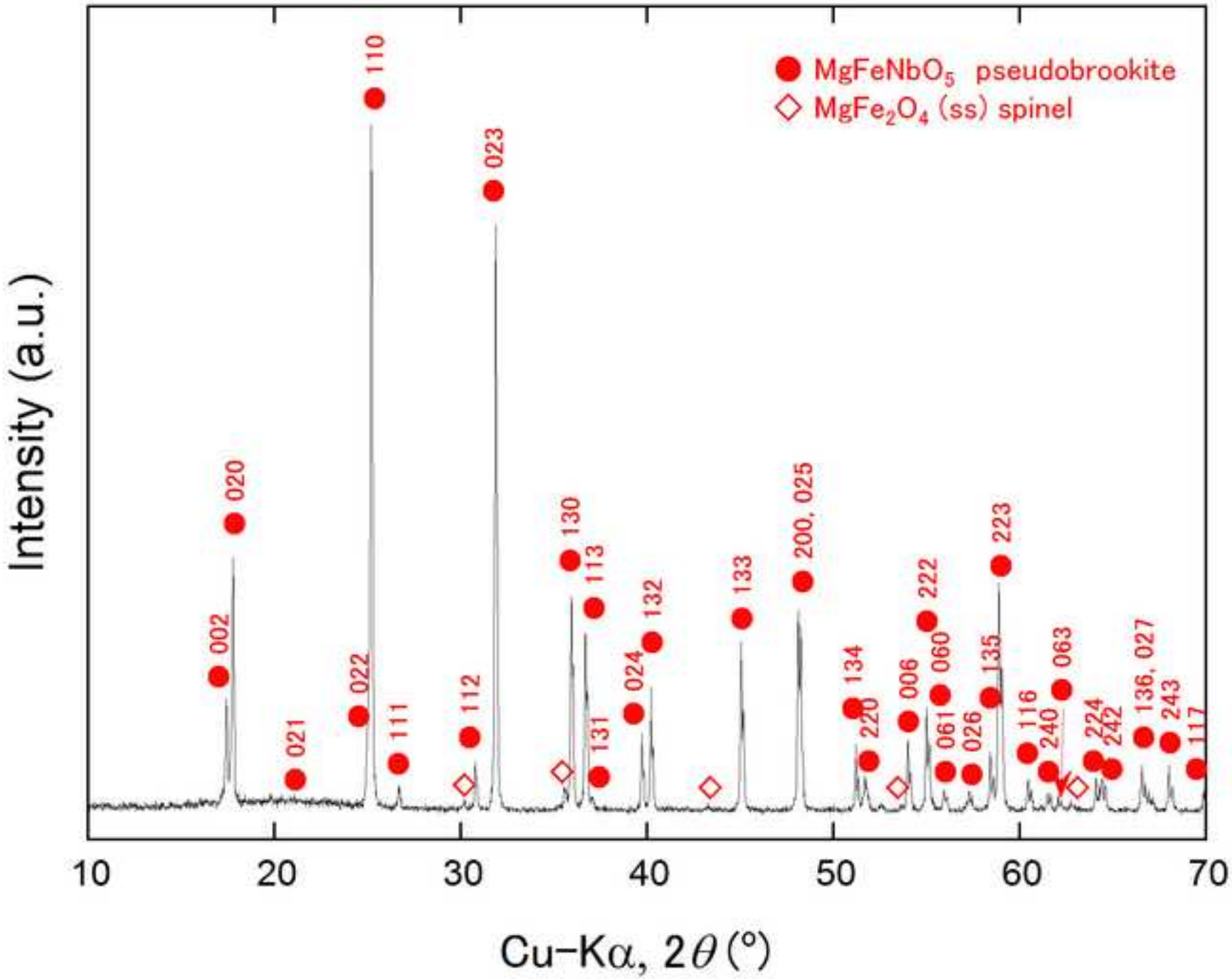

**Figure5**

**Click here to download high resolution image**

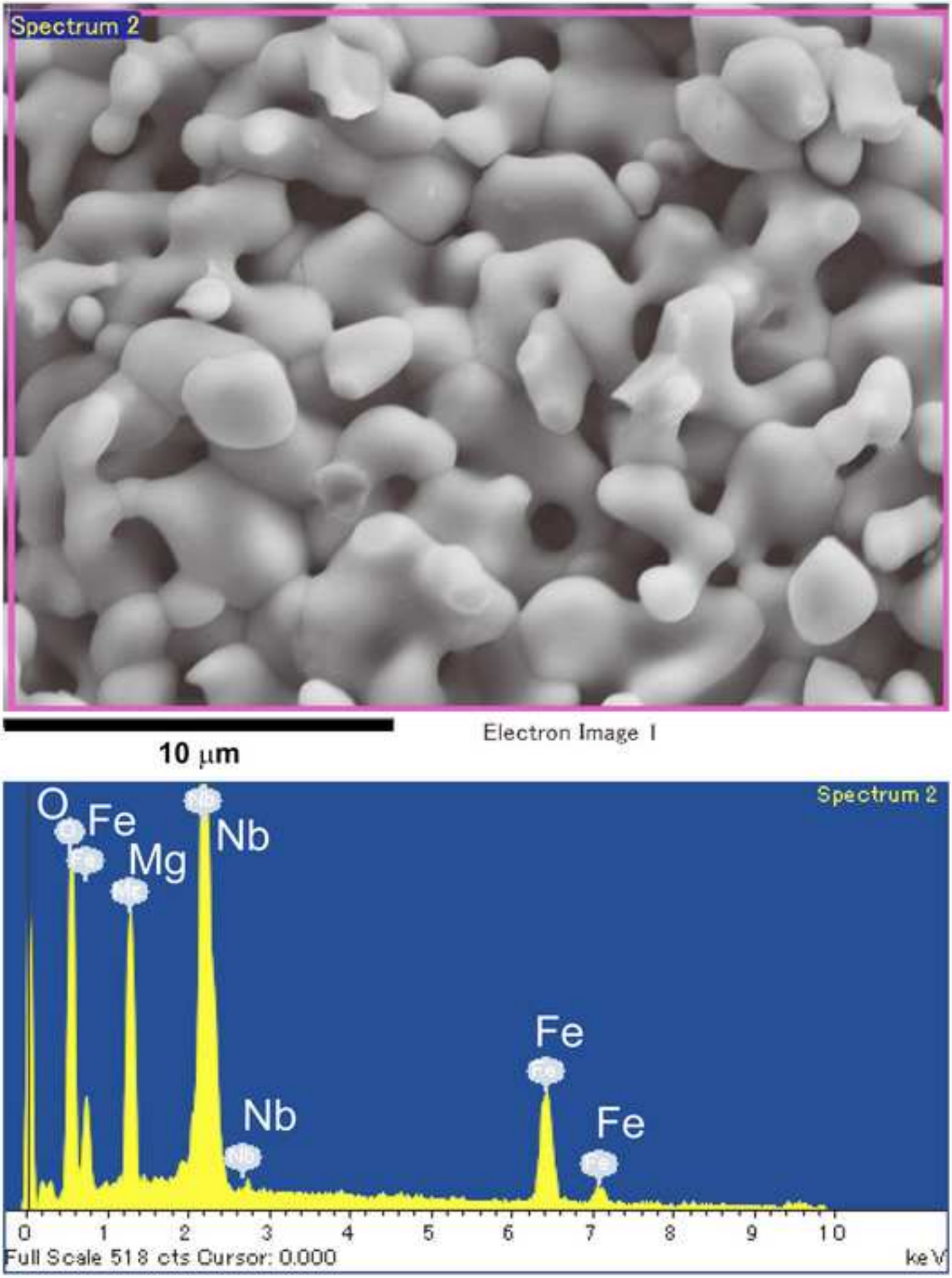

**Figure6**

**Click here to download high resolution image**

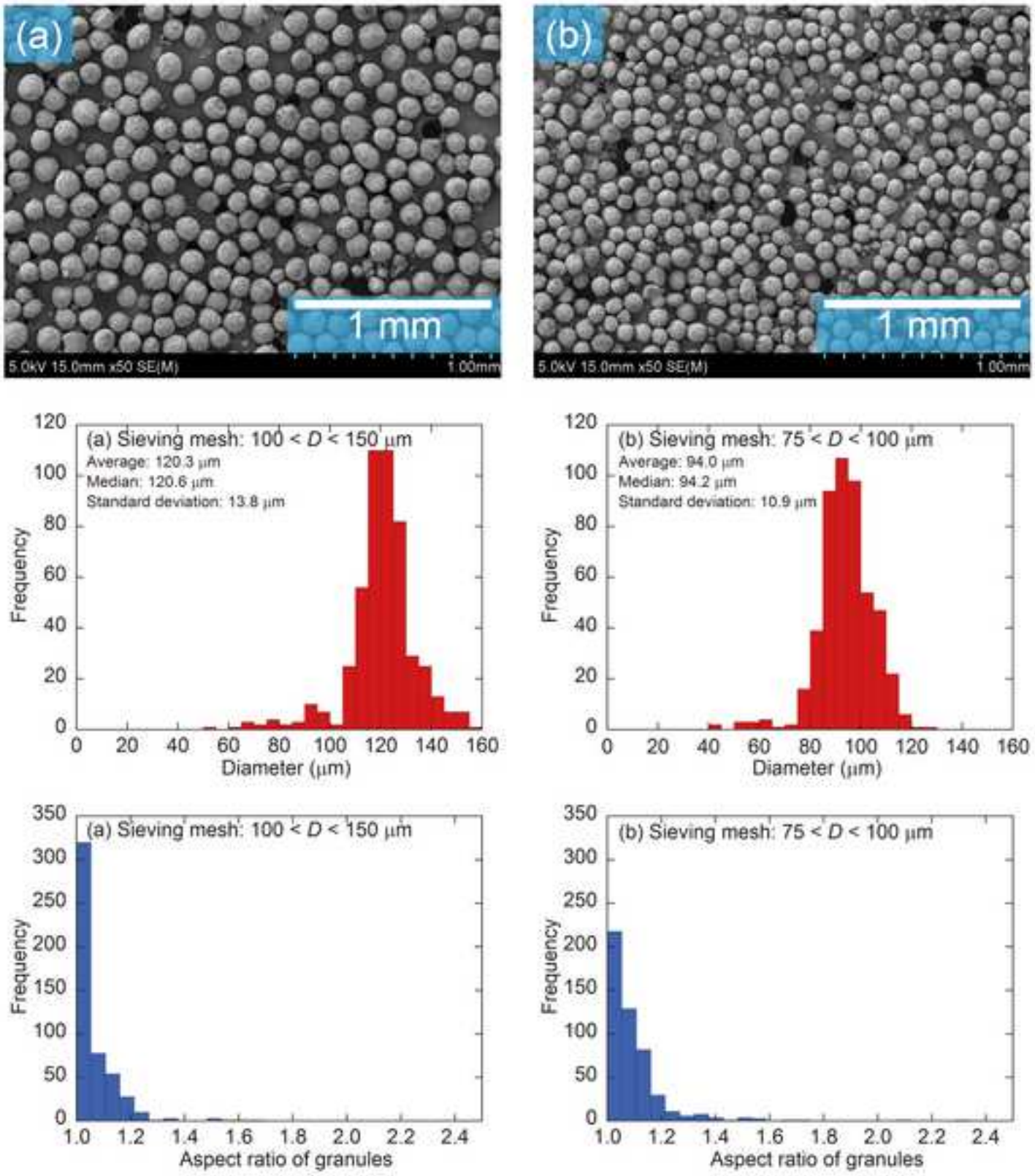

Figure7
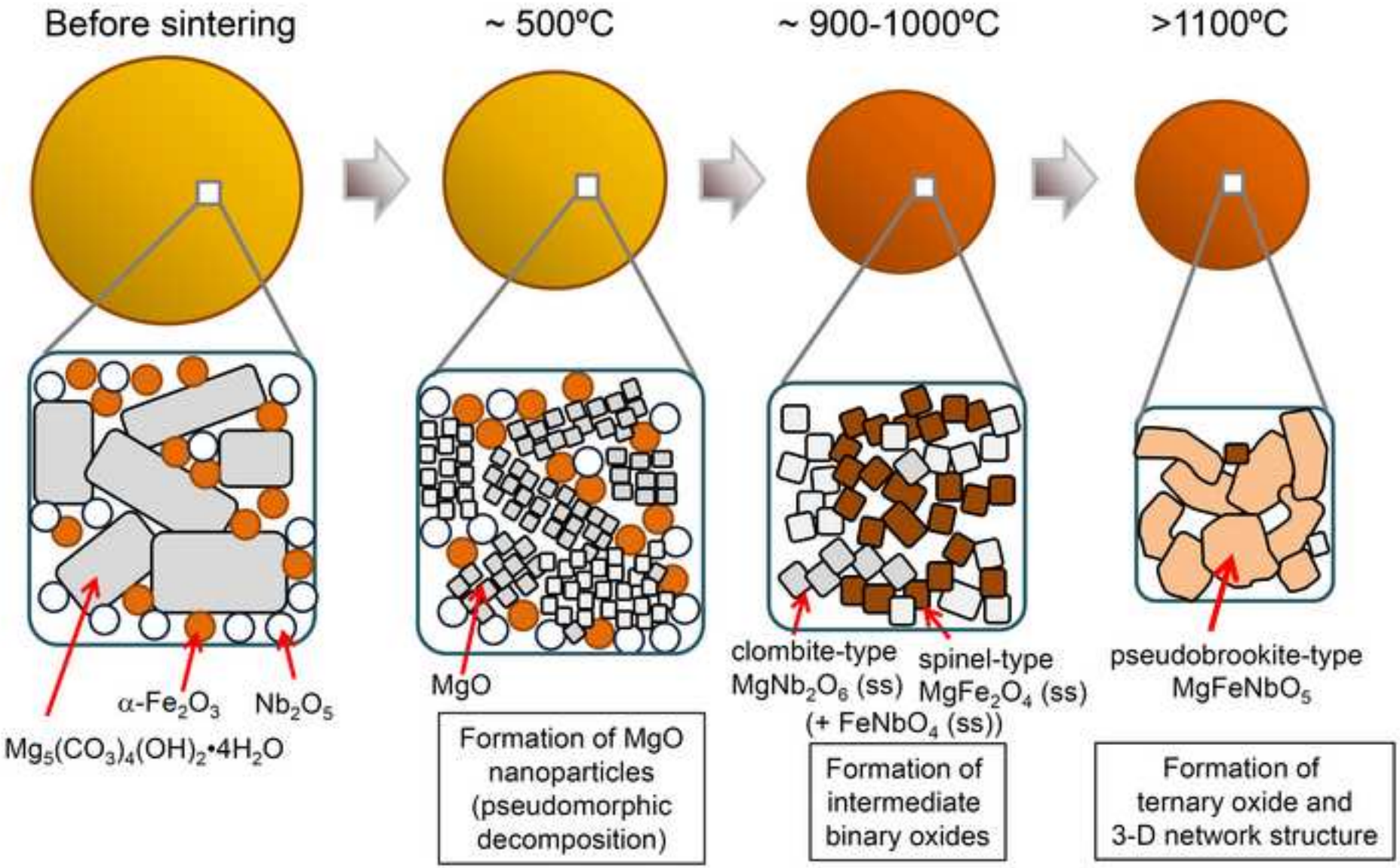
Click here to download high resolution image